



June 2003

Leaders in Cutting Edge Technology

Software, Hardware and Services for The Engineering Community



LEAP
Australia

Altair
Western Region US

DYNAMAX
US

Cril Technology
Simulation
France

GISSETA
India

MFAC
Canada

DYNAmore
Germany

Flotrend
Taiwan

KOSTECH
Korea

ERAB
Sweden

THEME
Korea

ALTAIR
Italy

CAD-FEM
Germany

Numerica SRL
Italy

ANSYS
China

Dr. Ted. Belytschko
US

Dr. Bhavin V. Mehta
US

Dr. Taylan Altan
US

Dr. David Benson
US

Dr. Alexey L. Borovkov
Russia

Prof. Gennaro Monacelli
Italy

Prof. Ala Tabiei
US

Articles

04	ANSYS - Wire Manufacturer Proves High-Performance Wire Is not Money For Old Rope
07	JRI – Examples of JMAG - Studio
09	AMD – Success Story
11	Commercial Participants
12	Special Announcements – Events – Courses – News Page

LS-DYNA Presented Publication

Two-Stage Stochastic and Deterministic Optimization

Editor	Trent Eggleston
Editor – Technical Content	Arthur B. Shapiro
Technical Writer	Dr. David Benson
Technical Writer	Uli Franz
Graphic Designer	Sandy Boling
Graphic Designer	Wayne Mindle
Feature Director	Marsha J. Victory

The contents of this publication is deemed to be accurate and complete. However, FEA Information Inc. doesn't guarantee or warranty accuracy or completeness of the material contained herein. All trademarks are the property of their respective owners. This publication is published for FEA Information Inc., copyright 2003. All rights reserved. Not to be reproduced in hardcopy or electronic copy.

Wire Manufacturer Proves High-Performance Wire Is Not Money For Old Rope
Copyright © Ansys, Inc.
Reprinted from the website www.ansys.com

Challenge: Conduct a structural contact analysis of steel rope terminations for anchoring offshore oil platforms prior to casting

Solution: Use ANSYS® Mechanical for its strong nonlinear capabilities.

Benefits: Nonlinear material analysis predicted that the part would not fail. Resulting analysis provided additional information that would have been expensive and time-consuming to gain from prototype testing



Introduction:

Despite being a world leader in the manufacturing of specialized wire and high performance wire rope products, Bridon International – part of FKI plc, an international engineering group – is still required to provide customers with a validation analysis before they will accept delivery.

Recently, the company’s Doncaster operation required a structural contact analysis of steel rope terminations for anchoring offshore platforms before casting could take place. They turned to Croydon-based Integrated Design and Analysis Consulting (IDAC) to perform the solid modeling and nonlinear structural analysis of the designs

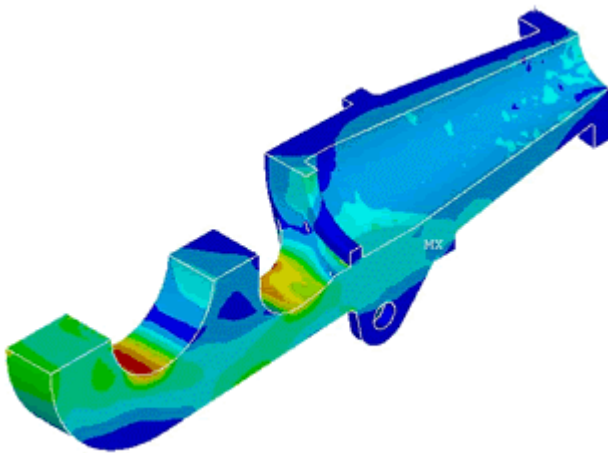
Challenge: The rope terminations are used in anchoring offshore oil platforms. Although similar designs are already used extensively in industry and have a proven ability to take operating loads, Bridon’s clients still require the validation analysis. Moreover, Bridon held detailed hand calculations for all models; nevertheless, analysis was needed for validation, as well as performance in the field having been proven.

The rope ends are single castings of more than a meter in length, the largest of which weighs well over a ton. The steel cable is inserted into the cavity of the casting, and then fixed in place with a setting resin to prevent it from sliding. With the socket fixed through a pinhole, it should be able to withstand cable loads of up to 5,000 kN in the case of the largest socket. Obviously, such large-scale components are not suited for easy prototyping. Also, the nature of offshore work demands safely designed parts, so accurate computer simulation offers a cost- and time-effective tool for the design process



Solution: Bridon supplied 2-D drawings of the three rope terminations, so that IDAC could create solid CAD models of the cast sockets and associated parts. The parts were imported directly into ANSYS Mechanical for the finite element analysis (FEA) stage. The model included nonlinear material properties for the steel parts to cater for any localized yielding that might be experienced. The resin, in which the steel rope was set inside, had directional material properties. IDAC modeled this behavior in ANSYS but no problems occurred.

The resin used in the sockets shrinks by up to 2% when it sets, therefore, a significant amount of movement is possible before the resin plug experiences any load. ANSYS contact capabilities cater to large displacements such as this, and also provide high-order surface contact elements that can represent complex surfaces such as the resin plug.



Load scenarios were run to predict the structural response at stages up to and including the breaking load of the cable. Separate load cases also were run for the different loads experienced during installation. Results indicated that the “closed-style” socket would withstand maximum loads without exceeding material stress limits. The two “open-style” sockets, however, could experience highly localized yielding as the breaking load of the cable was reached.

Benefits: The nonlinear material analysis predicted that plasticity redistributed stresses, and yielding did not continue through the section; therefore, part failure would not occur. This behavior suggested that through experience and previous calculations, Bridon had arrived at an optimal design with respect to material use. The sockets could safely endure the design loads

without using excess material. The FEA results confirmed this, and furthermore, provided valuable information in areas where it was difficult for hand calculations to represent all possible stresses.

While Bridon required validation of the rope terminations for their client, the resulting analysis provided additional information that would have been expensive and time-consuming to gain from prototype testing. The analysis acted as a valuable confirmation of their hand calculations, and also provided further insights into behavior such as stress distributions after yielding. With the analysis results, Bridon could proceed to the casting stage with increased confidence in their sockets and internal design procedures.

“The final report, being presented two weeks from instigation of the work, was presented professionally, and enabled Bridon to issue it directly to our customer with the addition of a very simple preface,” said Stuart Hallam, Technical Manager of Cable Products at Bridon International. “This report now has been accepted by both our customer and third party checking agency, allowing casting of the components to commence within the time frame set by the project team.”



ANSYS is a registered trademark and **DesignSpace** is a registered trademark of SAS IP, Inc., a wholly owned subsidiary of ANSYS Inc. All other trademarks and registered trademarks are the property of their respective owners.

The Japan Research Institute Ltd.

JMAG-Studio

A magnetic field analysis program that supports the development and design of electrical and electronic devices such as motors, actuators, circuit components, and antennas.

Applications include: Motors, Generators, Magnetization, Solenoids, Actuators, Transformers, Induction Heating, Magnetic Recording, Non-Destructive Testing, Superconductors, Antennas, Printed Circuit Boards, Electronic Devices, Electromagnetic Shields, Magneto-Optical Recording, Resonators, Displays, Printers, and many more.

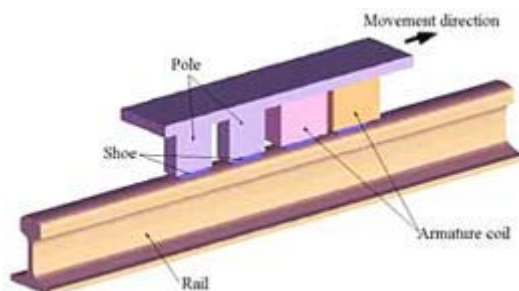
Analysis Functions Include: Magnetic Field Analysis, Electromagnetic Wave Analysis, Thermal Analysis, Electric Field Analysis, Structural Analysis. Coupled Analysis combining electromagnetic and thermal or structural analysis

For Complete Information and Examples Visit:

www.jri.co.jp/pro-eng/jmag/e/jmg/index.html

JMAG Analysis Examples:

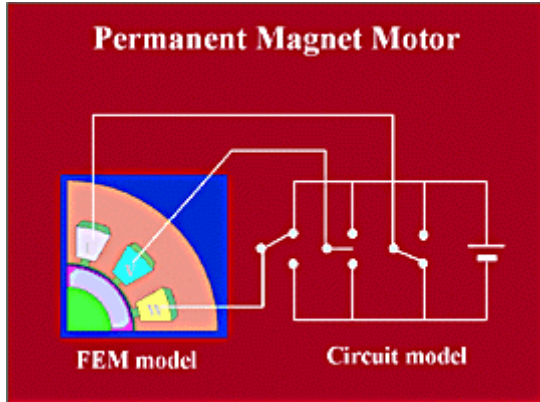
Velocity Electromotive Force Problem:



This example shows how JMAG can be used for the analysis of an eddy current brake for railcars. The brake shoe is enclosed in a coil, forming an electromagnet. If current is applied when the vehicle is traveling at speed, eddy currents are generated in the rail by means of the velocity electromagnetic force (VXB), producing an electromagnetic braking force. Since the rails are magnetic, the skin layer where eddy currents are generated is very thin when the railcar is traveling at high speed. A fine mesh division is therefore needed in the analysis model, which means that a large number of elements are required for an accurate model.

Velocity electromotive force problems are often thought to be unstable and the large-scale model required is extremely difficult to deal with. JMAG provides solutions through its unique development using a motional coordinate system and iterative calculation. In addition, modeling is simplified in this example since it is not necessary to move the meshes.

Coupled Analysis of Magnetic Fields and Electrical Circuits

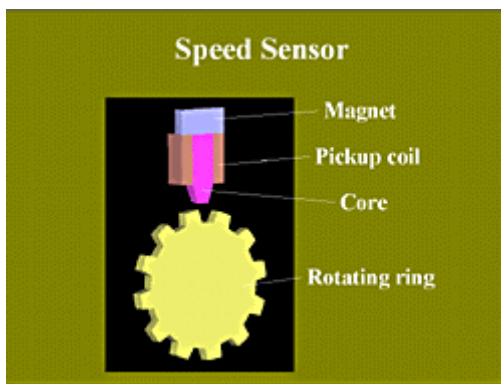


Analysis of PM motor activated by switching

In the analysis of electrical and electronic devices, considering the circuits that control the devices allows for a more sophisticated and realistic simulation. There are some cases where analysis may not be possible without coupled analysis of circuits and motion. For example, coupled analysis is essential in for PM motors that are activated by the switching operation of a three-phase square-wave voltage, as shown in the figure.

JMAG performs a complete coupled analysis by connecting circuits consisting of resistors, capacitors, coils, or switches, to a FEM model. Also, since motion can be incorporated using BEM or a sliding interface, realistic analysis of motors and actuators is possible. In this example, with a 1/4-size model due to its symmetry, analysis is conducted until the torque and electric current reach steady state condition

Analysis of a speed sensor



Magnetic flux reaches the rotary ring through the core

The number of revolutions of the rotary ring is detected from voltage signals produced by a pickup coil. The magnetic flux generated in the magnet reaches the rotary ring through the core.

Both core and rotary ring are made of magnetic material. Since the rotary ring is serrated like a gear, when it rotates, the distance from the core varies, changing the permeance of the magnetic circuit. This in turn changes the magnetic flux passing through the core, producing an electromagnetic force

Participant Success Story

Category: Pharmaceuticals
“virtual screening’ of small molecule libraries”

AMD - Aventis

Copyright © March 18, 2003, Reprinted from the website www.amd.com

““We're excited about the potential of powerful computing clusters. It's making a substantial difference in the way we do research.””

For Aventis, a world leader in the discovery, development and marketing of innovative pharmaceutical products, technology integration is a key factor in reducing the time from early research to launching a new drug in the market. Reducing this development time can ultimately help bring innovative treatments for diseases, such as cancer and diabetes, to patients sooner.

The challenges facing Aventis and other pharmaceutical companies are daunting. The industry's rule of thumb is that it takes 10 to 15 years from initial research to commercial availability of a new drug. The time lag between the research idea and the market reality is compounded by uncertainty. Years can be invested in the development of drugs that are never brought to market.

Scientists at the company's research facility in Tucson, Arizona meet these challenges every day with help from significant investments in computer-assisted drug design. One investment currently showing great promise is a 34-node cluster computer developed by California-based PSSC Labs that features AMD Athlon™ MP processors. PSSC Labs has delivered AMD Athlon MP processor-based, high-performance Beowulf clusters to government, university and research facilities worldwide.

The AMD Athlon MP processor-based cluster system is helping researchers with the needle-in-a-haystack hunt to identify small molecules that will either inhibit or activate a targeted protein. Altering the functions of these proteins by identifying small molecules is the key to treating diseases, such as cancer and diabetes. If researchers begin with structural information of the target protein, they believe they can find the small molecules much more quickly by using computer-aided “virtual screening” tools during the early stages of research.

“Previously, researchers were limited by the speed with which ‘virtual screening’ of small molecule libraries was performed,” said Anil Nair, senior associate scientist at Aventis’ research facility. “With the AMD Athlon™ MP processor-based cluster, I can utilize parallel processing to work through myriad possibilities to eliminate the bad ones and find the best choice. We can perform a ‘virtual screen’ on 10,000 or more small molecules each day.”

The capacity of the AMD Athlon MP processor-based cluster to meet compute-intense challenges, such as sorting through the vast mathematical possibilities of molecular research, derives in large part from the performance of the floating-point engine within the processor. “There's no question that one of the great strengths of the AMD Athlon MP processor is its ability to crunch numbers,” said Alex Lesser, vice president of PSSC Labs. “We regularly recommend AMD processor-based systems to our customers who perform floating-point intensive calculations.”

Given the extended process of drug discovery, one critical measure of performance is reliability. “The AMD Athlon MP processor-based system has proven itself to be highly reliable and we’re very pleased,” Nair said.

Nair is eager to build upon the current increase in productivity by adding more nodes to his system, saying he plans to double the size in the coming year with the expectation that it will double researchers’ productivity.

“We’re excited about the potential of this very powerful new tool,” he said. “It’s making a substantial difference in the way we do research.”

* * * * *

© 2003 Advanced Micro Devices, Inc. All rights reserved. AMD, the AMD Arrow logo, AMD Athlon, and combinations thereof, are trademarks of Advanced Micro Devices, Inc. Other product names used are for identification purposes only and may be trademarks of their respective companies.

**FEA Information Participants
Commercial and Educational**

Headquarters	Company	
Australia	Leading Engineering Analysis Providers	www.leapaust.com.au
Canada	Metal Forming Analysis Corp.	www.mfac.com
China	ANSYS – China	www.ansys.comcn
France	Cril Technology Simulation	www.criltechnology.com
Germany	DYNAmore	www.dynamore.de
Germany	CAD-FEM	www.cadfem.de
India	GissEta	www.gisseta.com
Italy	Altair Engineering srl	www.altairtorino.it
Italy	Numerica srl	www.numerica-srl.it
Japan	The Japan Research Institute, Ltd	www.jri.co.jp
Japan	Fujitsu Ltd.	www.fujitsu.com
Japan	NEC	www.nec.com
Korea	THEME Engineering	www.lsdyna.co.kr
Korea	Korean Simulation Technologies	www.kostech.co.kr
Russia	State Unitary Enterprise - STRELA	www.ls-dynarusia.com
Sweden	Engineering Research AB	www.erab.se
Taiwan	Flotrend Corporation	www.flotrend.com
UK	OASYS, Ltd	www.arup.com/dyna
USA	INTEL	www.intel.com
USA	Livermore Software Technology	www.lstc.com
USA	Engineering Technology Associates	www.eta.com
USA	ANSYS, Inc	www.ansys.com
USA	Hewlett Packard	www.hp.com
USA	SGI	www.sgi.com
USA	MSC.Software	www.mscsoftware.com
USA	DYNAMAX	www.dynamax-inc.com
USA	AMD	www.amd.com
Educational Participants		
USA	Dr. T. Belytschko	Northwestern University
USA	Dr. D. Benson	Univ. California – San Diego
USA	Dr. Bhavin V. Mehta	Ohio University
USA	Dr. Taylan Altan	The Ohio State U – ERC/NSM
USA	Prof. Ala Tabiei	University of Cincinnati
Russia	Dr. Alexey I. Borovkov	St. Petersburg State Tech. University
Italy	Prof. Gennaro Monacelli	Prode – Elasis & Univ. of Napoli, Federico II

Special Announcements and Highlights of News Pages

Posted on FEA Information and archived one month on the News Page

May 05	FEA Web Site	Added to AVI library 33-26
	ETA	DYNAFORM
	HP	Compaq D315 business PC
	FLOTREND	Distributor in Taiwan
May 12	INTEL	The Intel® Itanium®
	FUJITSU	Stylistic ST4000 Tablet PC
	STRELLA	Distributor in Russia

Events & Courses from the Events page on www.feainformation.com

June 27	Optimization Workshop at DYNAmore (free of charge)	Germany
Oct 02-05	Int' Conference on CAE	Italy
Oct 14-15	The Japan Research Institute LS-DYNA & JMAG Users Conference	Japan
Oct 29-31	Testing Expo North America	USA
Nov 11	LS-DYNA Update Forum from DYNAmore (free of charge)	Germany
Nov 12 –14	CAD-FEM User Conference	Germany
Nov 18-19	MSC. Software Virtual Product Development Conf.	UK

Two-Stage Stochastic and Deterministic Optimization

Tim Rzesnitzek, *
Dr. Heiner Müllerschön, †
Dr. Frank C. Günther, *
Michał Wozniak*

Abstract

The purpose of this paper is to explore some interesting aspects of stochastic optimization and to propose a two-stage optimization process for highly nonlinear automotive crash problems.

In the first stage of this process, a preliminary stochastic optimization is conducted with a large number of design variables. The stochastic optimization serves the dual purpose of obtaining a (nearly) optimal solution, which need not be close to the initial design, and of identifying a small set of design variables relevant to the optimization problem.

In the second stage, a deterministic optimization using only the set of relevant design variables is conducted. The result of the preceding stochastic optimization is used as the starting point for the deterministic optimization.

This procedure is demonstrated with a van-component model (previously introduced in [1]) used for crash calculations. LS-OPT [4] is used due to its ability to perform both stochastic (Latin Hypercube) and deterministic optimization.

1 Stage I: Stochastic Optimization

Stochastic optimization is often performed using the Monte Carlo method, where each design variable is individually constrained to lie within a user-specified upper and lower bound. The input values for these design variables are then determined randomly within their respective bounds.

The Latin Hypercube method provided by LS-OPT is also a random experimental design process. Figure 1 illustrates the algorithm used for generating random values for a small set of design variables (in this case, t_1 through t_4). The range of each design variable is subdivided into n equal intervals, where n is the number of experiments (in this case, the number of experiments is 5). A set of input variables is then determined for each experiment by randomly selecting one of the n sub-divisions for each variable. Each sub-division may be used within only one single experiment, thus ensuring that the entire design space is covered.

The distribution of design points for the Monte Carlo and Latin Hypercube algorithms can be influenced by adding additional constraints based on response functions. This requires a response function that depends linearly on the design variables. The responses of a new

*DaimlerChrysler, Commercial Vehicles Analysis

†DYNAMore GmbH

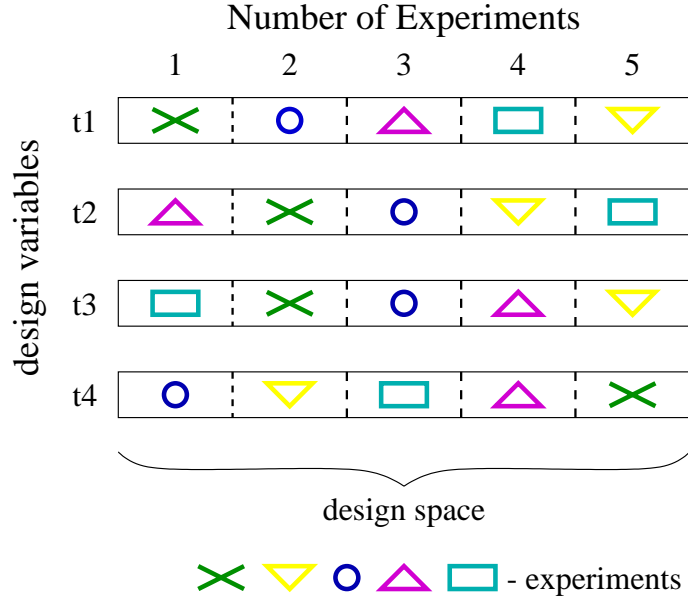


Figure 1: Latin Hypercube algorithm of LS-OPT

design can then be estimated by using the initial values of the design variables together with the corresponding initial responses.

For the optimization of a vehicle body, the mass of sheet metal parts linearly depends on sheet thickness, provided that the geometry remains unchanged. If the sheet thickness is a design variable, the mass for a new value of the sheet thickness can be estimated by multiplying the new sheet thickness by the ratio of initial sheet thickness to initial mass. Hence the total mass of all parts involved in an optimization can be estimated directly after the input values for an experiment are generated and can thus be used as a variable to define a constraint.

There are several different ways for enforcing the upper and lower bounds for a constraint variable:

1. In LS-OPT, a large number of initial design points is created. All points within this initial set exceeding the constraint are then shifted until they lie on the bound that has been exceeded. This is achieved, for example, by varying the sheet thicknesses appropriately. Depending on the number of points created for the initial set, a large number of design points may lie on the bounds of the constraint. Thus, in the second stage, the final set of design points is extracted from the initial set by the help of the D -optimality criterion [4].

The D -optimality criterion can be used with either a linear or quadratic approximation. The particular choice depends upon the equation applied to estimate the constraint variable from the design variables. If, for example, mass is defined as a constraint variable and the sheet thickness of each sheet metal part are the design variables, then linear approximation has to be used, since mass is linearly dependent from sheet thickness.

2. For the construction of a Monte Carlo design, experiments outside of the constraint are filtered out when the set of design points is created. The generation of random values for

a single experiment is repeated until a design is found for which the constraint variable meets the bounds.

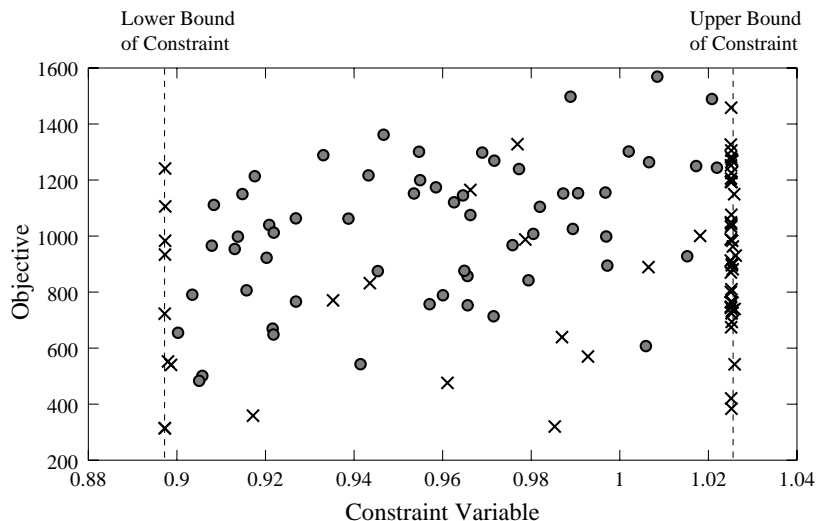


Figure 2: Distribution of design points for Latin Hypercube and the Monte Carlo algorithm

In the diagram of figure 2 the objective variable is plotted vs. the constraint variable for sets of design points generated by LS-OPT (Latin Hypercube) and the Monte Carlo algorithm. The design points produced by LS-OPT (x) often lie on the borders of the constraint, which results in an irregular distribution of the set of design points. Obviously the D -optimality criterion applied to extract the final set of design points from such an initial set does not strongly improve the distribution of the design points.

In contrast to Latin Hypercube, the set of design points created by the Monte Carlo algorithm shows the typical distribution of a random experimental design, where no design point is lying on a bound and the number of design points is decreasing towards the bounds according to a Gaussian distribution. Thus the number of design points suitable for analysis is large in comparison to Latin Hypercube.

Figure 3 illustrates the advantage of performing a constrained Monte Carlo design. Without any constraint, a simulation would be carried out for all the design points plotted on the diagram. By defining a constraint, the experiments that are uninteresting or irrelevant are effectively filtered out. Thus the number of simulations required can be reduced.

2 Stage II: Identifying Important Variables for Deterministic Optimization. Regression Analysis

2.1 General Concepts

In statistical literature, there are many different representations of the concepts involved in finding the underlying dependencies between input and output variables based on a number of experiments, e.g. [3]. Let us show one possible derivation:

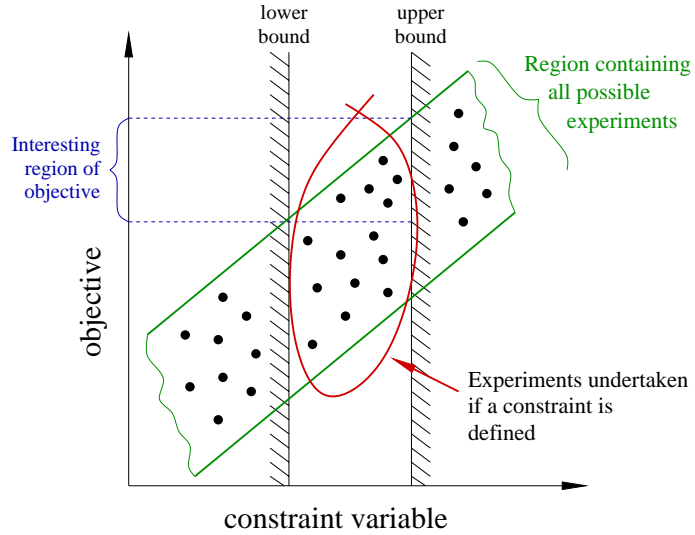


Figure 3: Definition of constraints for stochastic optimization

Let there be p experiments (simulations), each of which is characterized by an $n \times 1$ vector $\hat{\mathbf{x}}_i$ of input variables and one output variable \hat{y}_i . In crash simulations, $\hat{\mathbf{x}}_i$ could be a vector of sheet thicknesses and other parameters, and \hat{y}_i could be a measure of the crashworthiness of the resulting structure. There are several commercial software tools available that can generate p sets of input variables, and run p simulations to obtain output variables y_i . We used LS-OPT [4] as well as our own Perl [5] programs to generate the examples shown in Section 4.

Let us define a $n \times p$ matrix of all input values,

$$\hat{\mathbf{X}} = \begin{bmatrix} \hat{\mathbf{x}}_1 & \hat{\mathbf{x}}_2 & \dots & \hat{\mathbf{x}}_p \end{bmatrix}, \quad (1)$$

and a corresponding $1 \times p$ vector of output values,

$$\hat{\mathbf{y}}^T = \begin{bmatrix} \hat{y}_1 & \hat{y}_2 & \dots & \hat{y}_p \end{bmatrix}. \quad (2)$$

It is customary to center the values for $\hat{\mathbf{x}}_i$ and \hat{y}_i with their mean values over all experiments:

$$\bar{\mathbf{X}} = \hat{\mathbf{X}} - \frac{1}{p} \sum_{i=1,p} \hat{\mathbf{x}}_i = \hat{\mathbf{X}} - \frac{1}{p} \hat{\mathbf{X}} \mathbf{1}_{p \times p}, \quad (3)$$

where $\mathbf{1}_{p \times p}$ is a $p \times p$ matrix of ones. Analogously,

$$\bar{\mathbf{y}}^T = \hat{\mathbf{y}}^T - \frac{1}{p} \hat{\mathbf{y}}^T \mathbf{1}_{p \times p}. \quad (4)$$

Let us now define covariance matrices¹ for $\bar{\mathbf{X}}$ and $\bar{\mathbf{y}}^T$:

$$\mathbf{S}_x^2 = \bar{\mathbf{X}} \bar{\mathbf{X}}^T \quad (5)$$

$$S_y^2 = \bar{\mathbf{y}}^T \bar{\mathbf{y}}. \quad (6)$$

¹in statistical literature, covariance matrices usually contain a factor $\frac{1}{p}$. However, this is not necessary for our purposes.

It is easily established that \mathbf{S}_x^2 is positive semidefinite. In order to obtain the standard deviation² \mathbf{S}_x with

$$\mathbf{S}_x^2 = \mathbf{S}_x \mathbf{S}_x, \quad (7)$$

we can perform an eigenvalue decomposition³ of \mathbf{S}_x^2 and take the square roots of the eigenvalues, viz.

$$\mathbf{S}_x^2 = \mathbf{T}^T \mathbf{diag} \{ \lambda_i \} \mathbf{T} \quad (8)$$

$$\mathbf{S}_x = \mathbf{T}^T \mathbf{diag} \left\{ \sqrt{\lambda_i} \right\} \mathbf{T} \quad (9)$$

$$\lambda_i \geq 0 \quad \text{due to positive semidefiniteness.} \quad (10)$$

Of course,

$$S_y = \sqrt{S_y^2} \quad (11)$$

is computed trivially.

Let us now introduce the transformed variables

$$\mathbf{X} = \mathbf{S}_x^{-1} \bar{\mathbf{X}} \quad (12)$$

$$\mathbf{y}^T = S_y^{-1} \bar{\mathbf{y}}^T, \quad (13)$$

assuming \mathbf{S}_x is invertible and $S_y \neq 0$. These variables are normalized in the sense that

$$\mathbf{X} \mathbf{X}^T = \mathbf{S}_x^{-1} \bar{\mathbf{X}} \bar{\mathbf{X}}^T \mathbf{S}_x^{-1} = \mathbf{S}_x^{-1} \mathbf{S}_x^2 \mathbf{S}_x^{-1} = \mathbf{I} \quad (14)$$

$$\mathbf{y}^T \mathbf{y} = S_y^{-1} \bar{\mathbf{y}}^T \bar{\mathbf{y}} S_y^{-1} = S_y^{-1} S_y^2 S_y^{-1} = 1. \quad (15)$$

Our goal is to find a linear approximation with a $n \times 1$ vector \mathbf{w} such that the residual

$$\mathbf{r} = \mathbf{y} - \mathbf{X}^T \mathbf{w} \quad (16)$$

is minimized. Minimizing the quadratic norm of \mathbf{r} is equivalent to minimizing $\mathbf{r}^T \mathbf{r}$, hence the name Least Squares Approximation.

With the orthogonality conditions 14 and 15, we obtain

$$\mathbf{r}^T \mathbf{r} = (\mathbf{y}^T - \mathbf{w}^T \mathbf{X}) (\mathbf{y} - \mathbf{X}^T \mathbf{w}) \quad (17)$$

$$= \mathbf{y}^T \mathbf{y} - \mathbf{y}^T \mathbf{X}^T \mathbf{w} - \mathbf{w}^T \mathbf{X} \mathbf{y} + \mathbf{w}^T \mathbf{X} \mathbf{X}^T \mathbf{w} \quad (18)$$

$$= 1 - 2\mathbf{w}^T \mathbf{X} \mathbf{y} + \mathbf{w}^T \mathbf{w} \quad (19)$$

In index notation, this becomes

$$r_i r_i = 1 - 2w_i X_{ij} y_j + w_i w_i, \quad (20)$$

where summation over double indices is implied.

The minimum of equation 20 can be found by taking the derivative with respect to \mathbf{w} and setting it to zero. In index notation:

$$\frac{\partial (r_i r_i)}{\partial w_k} = -2\delta_{ik} X_{ij} y_j + \delta_{ik} w_i + w_i \delta_{ik} \quad (21)$$

$$= -2X_{kj} y_j + 2w_k = 2(w_k - X_{kj} y_j). \quad (22)$$

²Give or take a factor $\frac{1}{\sqrt{p}}$.

³This process is significantly simplified if the input variables \mathbf{x} are completely independent of each other. In such a case, the covariance matrix becomes diagonal: $\mathbf{S}_x^2 = \mathbf{diag} \{ \lambda_i \}$ and $\mathbf{T} = \mathbf{I}$, hence $\mathbf{S}_x = \mathbf{diag} \{ \sqrt{\lambda_i} \}$

The Kronecker delta δ_{ij} is defined as

$$\delta_{ij} = \begin{cases} 1 & \text{if } i = j \\ 0 & \text{otherwise.} \end{cases} \quad (23)$$

Back in matrix notation, we find that

$$\mathbf{w} = \mathbf{X}\mathbf{y}. \quad (24)$$

Our linear approximation becomes

$$y = \mathbf{w}^T \mathbf{x} = \mathbf{y}^T \mathbf{X}^T \mathbf{x}. \quad (25)$$

This gives rise to interpreting the elements of \mathbf{w} as the significance of each normalized input variable in the vector

$$\mathbf{x} = \mathbf{S}_x^{-1} \bar{\mathbf{x}} \quad (26)$$

for the result of the simulation. Generally, the elements of \mathbf{x} are a linear combination of the elements of $\bar{\mathbf{x}}$.

In terms of centered variables 3 and 4 we obtain

$$\bar{y} = \underbrace{\bar{\mathbf{y}}^T \bar{\mathbf{X}}^T}_{\bar{\mathbf{w}}} (\bar{\mathbf{X}} \bar{\mathbf{X}}^T)^{-1} \bar{\mathbf{x}}. \quad (27)$$

The weight vector $\bar{\mathbf{w}}$ contains the non-normalized regression coefficients. Hence, its values cannot be compared to each other directly.

2.2 Variable Screening in LS-OPT (ANOVA)

LS-OPT provides the capability of performing a significance test for each variable in order to remove those coefficients or variables which have a small contribution to the design model [4]. For each response, the variance of each variable with respect to that response is tracked and tested for significance using the partial F-test [2]. The importance of a variable is penalized by both a small absolute coefficient value (weight) computed from the regression, as well as by a large uncertainty in the value of the coefficient pertaining to the variable. A 90% confidence level is used to quantify the uncertainty and the variables are ranked based on this level.

The $100(1 - \alpha)\%$ confidence interval for the regression coefficients b_j , $j = 1, \dots, n$ is determined by

$$b_j - \frac{\Delta b_j}{2} \leq \beta_j \leq b_j + \frac{\Delta b_j}{2} \quad (28)$$

where

$$\Delta b_j = 2 t_{\alpha/2, p-(n+1)} \sqrt{\hat{\sigma}^2 C_{jj}} \quad (29)$$

and $\hat{\sigma}^2$ is an unbiased estimator of the variance σ^2 given by

$$\hat{\sigma}^2 = \frac{\varepsilon^2}{p - (n + 1)} = \frac{\sum_{i=1}^p (y_i - \hat{y}_i)^2}{p - (n + 1)} \quad (30)$$

C_{jj} is the diagonal element of $(\hat{\mathbf{X}}^T \hat{\mathbf{X}})^{-1}$ corresponding to b_j and $t_{\alpha/2, p-(n+1)}$ is the t or Student's Distribution. ε is the error between the response y_i and the estimated response \hat{y}_i

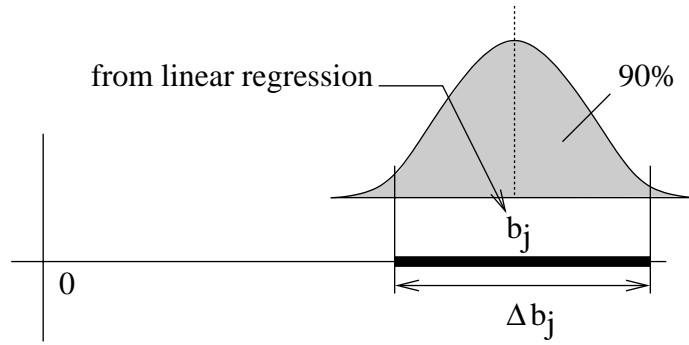


Figure 4: Confidence interval for the regression coefficient for variable j

evaluated by linear regression. $100(1 - \alpha)\%$ therefore represents the level of confidence that b_j will lie within the computed interval, (4).

Figure 5 demonstrates graphically the criterion for the ranking of the variables. A 90% confidence level defines the lower bound and the variables are ranked according to this lower bound. If the lower bound is less than zero, the variable is declared as insignificant.

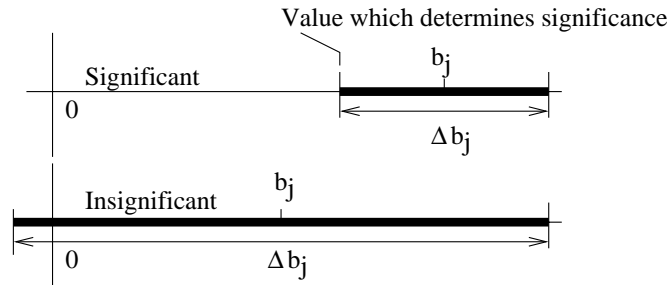


Figure 5: Criterion for the significance of a variable

Each variable is normalized with respect to the size of the design space. Thus all variables range within the interval $[0,1]$ and a reasonable comparison can be made for variables of different kinds.

3 Description of Van Component Model for Crash

The scope of the optimization is an assembly of a vehicle body for a commercial van as shown in Figure 6.

The main components of that assembly are the first cross member and the front part of the longitudinal member of the frame. Furthermore, the absorbing box between first cross member and longitudinal member, parts of the wheelhouse and the closing panels of the longitudinal member are also included in the assembly.

In Figure 7, boundary conditions and part numbers of important components are illustrated.

The assembly is connected to the bottom sheet of the vehicle body at the flanges of the front and back closing panels. In the simulations, the assembly is fixed in y - and z -directions

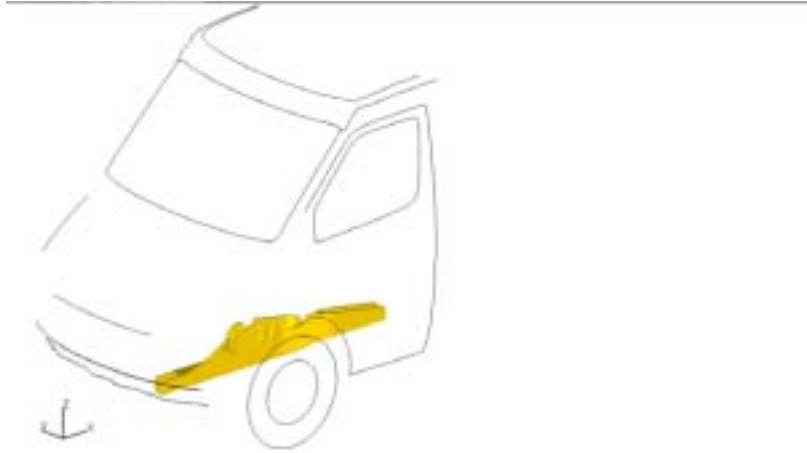


Figure 6: Position of the assembly within the vehicle

at these flanges. The assembly is displaced in x-direction at a constant velocity and deforms at the stonewall.

For simulation purposes, only half of the frame is represented (since geometry and loads are symmetric to the yz-plane) and the first cross member is cut off at the yz-plane. Therefore, the translation in the y-direction and the rotation about the x- and z-axis have to be fixed along the cutting edge.

4 Application of Concepts to the Example Model

A two-stage optimization has been performed for the component model described above. In the first stage, two different kinds of random distributions are applied in order to generate samples of design variables. The two methods are a *Monte Carlo* distribution provided by a perl program and a *Latin Hypercube* design combined with D-Optimal strategy provided by LS-OPT. The two approaches are compared to each other.

In the second stage, a deterministic optimization using the successive response surface methodology of LS-OPT is performed. The start design for this is the best set of variables resulting out of the first stage.

4.1 Description of the optimization problem

The design variables consists of the sheet thicknesses of 15 parts and an additional bead located on the longitudinal member on the outer and inner side. The geometry and the location of the bead is identical on both sides (symmetry). The bead is defined by 5 design variables, the depth t , the x-location x_{min}, x_{max} and the z-location z_{min}, z_{max} . Preprocessing of the LS-DYNA input file for the bead is done by a Perl program (for additional information, see [1]). In total there are 20 design variables.

The objective of the optimization is to maximize the ratio of the maximum value of the internal energy E_{max} and the mass M of the considered components:

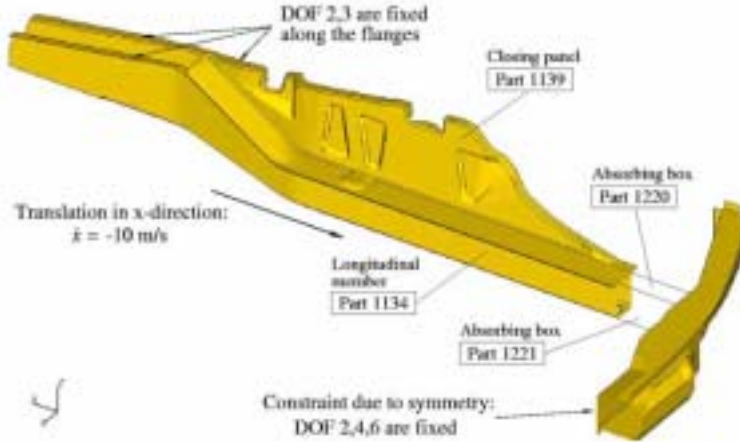


Figure 7: Boundary Conditions

$$E_M = \frac{E_{\max}}{1000 M} \longrightarrow \max E_M. \quad (31)$$

Two constraints are required to be fulfilled:

- Bounds for the Mass: $0.895 > M > 1.022$
- Upper bound for the stonewall force: $\max\text{RWFORC} = 1.25$

For the evaluation of the maximum rigid wall force, $\max\text{RWFORC}$, the history curve (ASCII-file `RWFORC`) is filtered using SAE 180.

4.2 Stage I: *Monte Carlo* and *Latin Hypercube* Distributions

4.2.1 *Monte Carlo* Distribution

In the first attempt, 60 simulations with 60 different sets of input variables are performed. Variable sets are generated by a Perl programm using a modul for generating random values. The total mass of the component model is checked directly and sets that are outside the specified bounds are rejected. This is done until 60 feasible variable sets are available.

The three runs with the maximum ratio E_M and with a stonewall force less than 1.5 are chosen to be the starting values for 15 additional runs each. Thus, three sets of 15 variables vary their values with these starting values as centerpoints. This is repeated for the three best points of the previous 45 runs with $3 \times 15 = 45$ more runs.

Thus, in total $1 \times 60 + 3 \times 45 + 3 \times 45 = 150$ runs are put into execution.

4.2.2 *Latin Hypercube* Distribution

The *Latin Hypercube* design is provided by LS-OPT. LS-OPT generates an initial 1000 *Latin Hypercube* points (sets of variables, see Section 1). Points that violate the mass constraint are moved automatically into the feasible mass region. Out of these 1000 feasible points, a sub-set

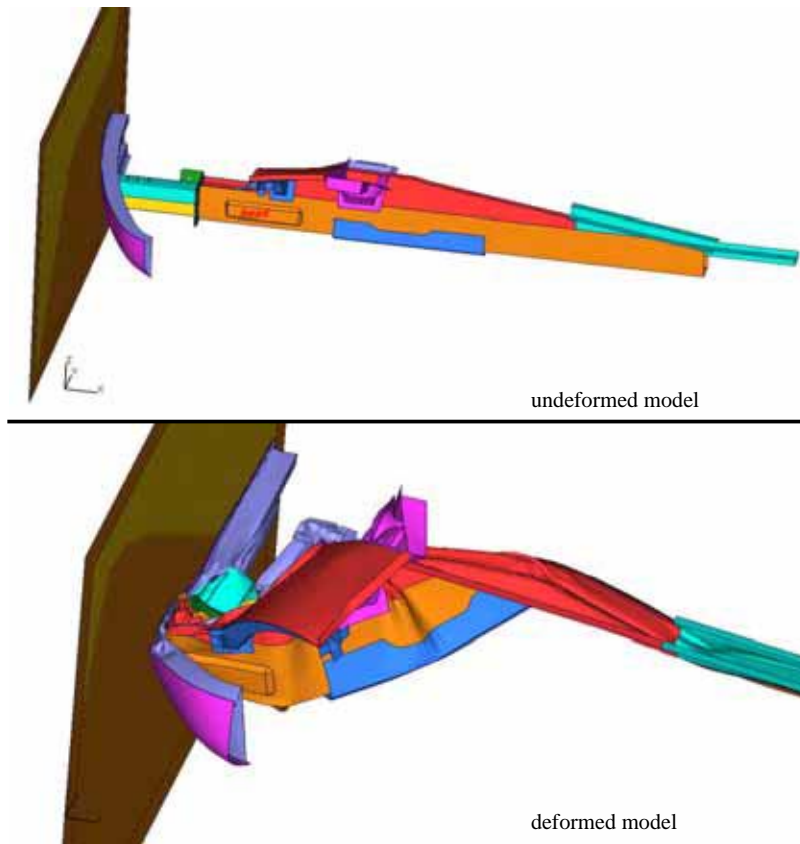


Figure 8: Simulation model - initial and deformed configuration

of 60 points is selected by applying the D-Optimal criterion (see [4]). Points chosen by the D-Optimal criterion generally display good capabilities with respect to linear regression.

In the same manner, 30 more points are generated using as the centre point the best run out of the first 60 runs.

Thus, in total $1 \times 60 + 1 \times 30 = 90$ runs are put into execution.

4.3 Stage II: Deterministic Optimization using LS-OPT

In order to reduce the amount of variables for the deterministic optimization in Stage II, an ANOVA analysis (Section 2.2) is performed. Therefore, the first 60 runs of the *Latin Hypercube* Distribution are used. Figure 9 shows the results of the variable screening. LS-OPT ranks the variables by using the bound of the 90% confidence interval that is closest to zero as the ranking number.

The four most significant variables t_{1134} , t_{1139} , t_{1210} and t_{1221} are chosen for the deterministic optimization using the response surface method in LS-OPT. For the starting variables the values are taken out of the best run of the 150 *Monte Carlo* simulations. The values of the remaining 16 variables are also taken out of the optimal *Monte Carlo* run and are kept constant. It is slightly surprising, that in the third iteration no improvement of E_M is observed (Figure 10). Thus, the starting value for the deterministic optimization comes from

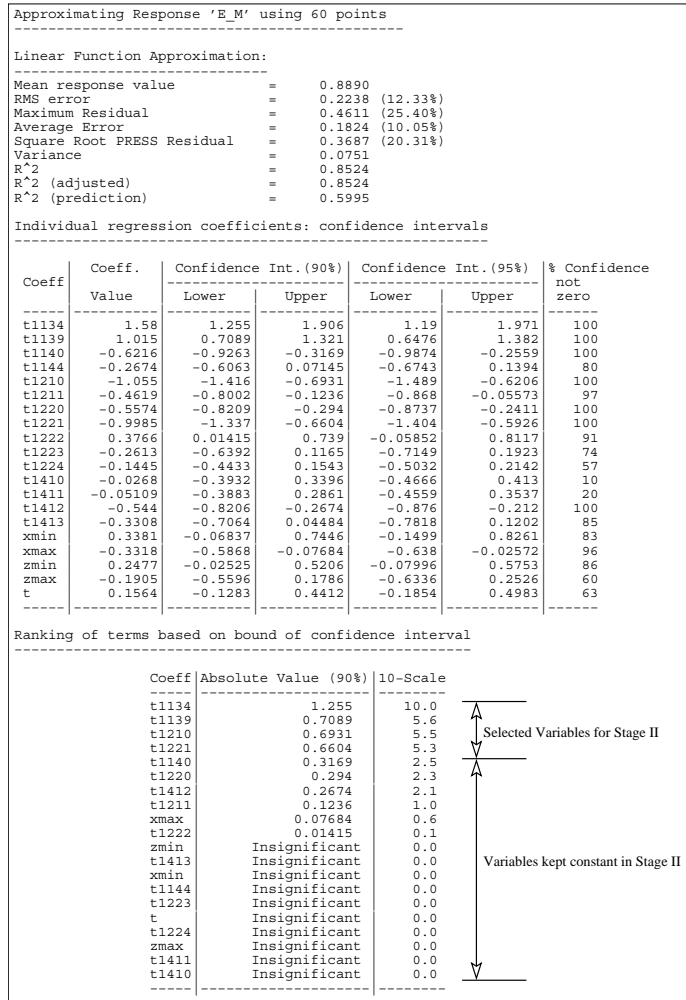


Figure 9: Output of LS-OPT for variable screening with respect to the response E_M

the sample distribution of the second iteration. Within the *Latin Hypercube* samples, the best result with respect to the maximum Energy-Mass ratio E_M is significantly worse than the best result for the *Monte Carlo* samples (compare Figure 10). This is probably due to the movement of the variables in order to fulfill the mass constraints. This leads to a degenerated sample distribution with an accumulation of samples at the lower and upper bound of the mass constraints (Figure 2).

Figure 10 shows the results of the *Monte Carlo* and the *Latin Hypercube* simulations of Stage I and the result of an optimum run found by LS-OPT using the response surface methodology in Stage II. A significant additional improvement of the response E_M by the deterministic approach is observed.

5 Conclusions

The present paper shows the proceeding of a two-stage optimization, where in the first stage a stochastic approach is considered and in the second stage, starting from the best result of the first stage, a deterministic optimization using the Response Surface Method in LS-OPT is performed.

The variation of the design variables (sheet thicknesses) is restricted by a mass constraint. This is done in order to achieve only samples whose mass lies within a desired range. This ensures that needless simulations are avoided.

On the basis of a set of *Latin Hypercube* simulations, a variable screening using the ANOVA (ANalysis Of VAriance) feature in LS-OPT is performed. With this tool, those variables detected as insignificant are removed for the second stage of the optimization process.

The starting variables for the deterministic optimization in the second stage are taken out of the best run of the *Monte Carlo* simulations. A significant additional improvement of the Energy/Mass ratio by the deterministic approach is observed. In total, an improvement of 32.78 % from the initial configuration (1.205) to the optimum result of LS-OPT (1.60) is achieved (Figure 10).

The combination of stochastic and deterministic optimization has shown to be a reasonable method for obtaining sensible input values for a deterministic optimization. Furthermore, it can be expected that in many cases, the convergence of the deterministic algorithm to local extremal values with respect to the objective may be avoided.

References

- [1] F. Günther and T. Rzesnitzek. Crashworthiness optimization of van components with ls-opt. In *Proceedings of 19th CAD-FEM Users' Meeting*, 2001.
- [2] R. Myers and M. D.C. *Response Surface Methodology*. Wiley New York, 1995.
- [3] H. Rinne. *Statistische Analyse multivariater Daten: Einführung*. R. Oldenbourg Verlag München Wien, 2000.
- [4] N. Stander and K. Craig. *LS-OPT User's Manual: Design Optimization Software for the Engineering Analyst*. Livermore Software Technology Corporation, 2002.
- [5] L. Wall, T. Christiansen, and J. Orwant. *Programming Perl*. O'Reilly & Associates, 3rd edition, 2000.

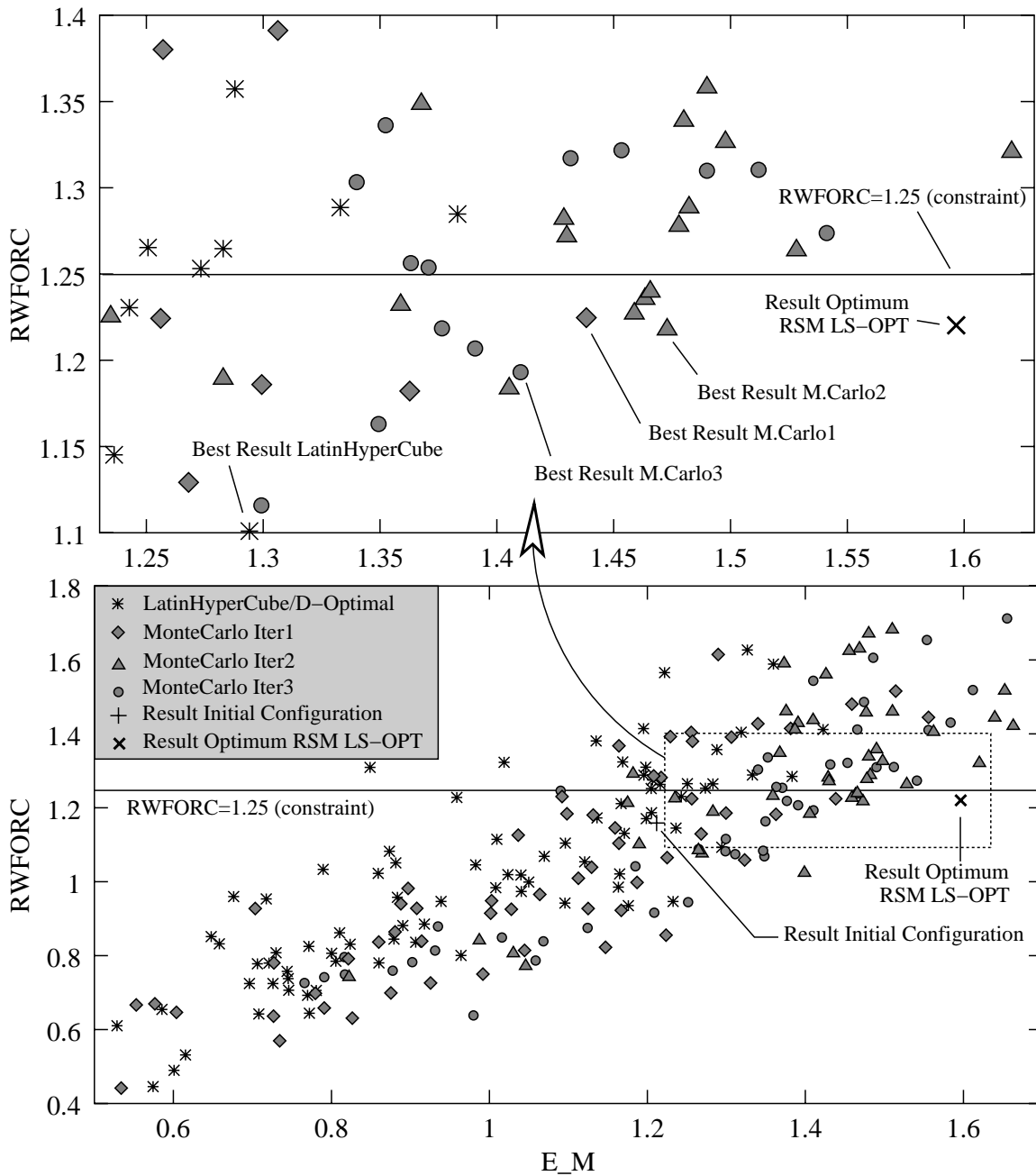


Figure 10: Response E_M vs. the corresponding rigid wall force RWFORC for *Latin Hypercube* and *Monte Carlo* Samples and for the final optimum found by the Response Surface Method (RSM) in Stage II